Temperature-driven single-valley Dirac fermions in HgTe quantum wells

M. Marcinkiewicz,[1] S. Ruffenach,[1] S. S. Krishtopenko,[1,2] A. M. Kadykov,[1,2] C. Consejo,[1] D. B. But,[1] W. Desrat,[1] W. Knap,[1,3] J. Torres,[4] A. V. Ikonnikov,[2] K. E. Spirin,[2] S. V. Morozov,[2,5] V. I. Gavrilenko,[2,5] N. N. Mikhailov,[6,7] S. A. Dvoretskii,[6,7] and F. Teppe[1,*]

[1]*Laboratoire Charles Coulomb, UMR Centre National de la Recherche Scientifique 5221, University of Montpellier, F-34095 Montpellier, France*

[2]*Institute for Physics of Microstructures RAS, GSP-105, Nizhni Novgorod 603950, Russia*

[3]*Institute of High Pressure Physics, Polish Academy of Sciences, Sokołowska 29/37, PL-01-142 Warsaw, Poland*

[4]*Institut d'Electronique et des Systemes, UMR Centre National de la Recherche Scientifique 5214, University of Montpellier, F-34095 Montpellier, France*

[5]*Lobachevsky State University of Nizhni Novgorod, prospekt Gagarina 23, Nizhni Novgorod 603950, Russia*

[6]*Institute of Semiconductor Physics, Siberian Branch, Russian Academy of Sciences, prospekt Akademika Lavrent'eva 13, Novosibirsk 630090, Russia*

[7]*Novosibirsk State University, Pirogova Street 2, Novosibirsk 630090, Russia*

(Received 22 February 2017; published 5 July 2017)

We report on the temperature-dependent magnetospectroscopy of two HgTe/CdHgTe quantum wells below and above the critical well thickness d_c. Our results, obtained in magnetic fields up to 16 T and s temperature range from 2 to 150 K, clearly indicate a change in the band-gap energy with temperature. A quantum well wider than d_c evidences a temperature-driven transition from topological insulator to semiconductor phases. At a critical temperature of 90 K, the merging of inter- and intraband transitions in weak magnetic fields clearly specifies the formation of a gapless state, revealing the appearance of single-valley massless Dirac fermions with a velocity of 5.6×10^5 m s^{-1}. For both quantum wells, the energies extracted from the experimental data are in good agreement with calculations on the basis of the eight-band Kane Hamiltonian with temperature-dependent parameters.

DOI: 10.1103/PhysRevB.96.035405

Within the last decade, realizations of massless Dirac fermions (DFs) have been extensively studied in condensed matter systems [1]. This study began with the discovery of graphene hosting two-dimensional (2D) massless DFs coming from two nonequivalent valleys [2,3]. Since then, 2D and 3D massless fermions have also been identified at the surfaces of 3D topological insulators (TIs) [4] and in Dirac and Weyl semimetals [5–8]. HgTe-based quantum wells (QWs) were the first 2D systems after graphene, in which massless DFs were experimentally demonstrated [9]. As the QW width d is varied, the first electronlike subband ($E1$) crosses the first holelike subband ($H1$) [10,11]. When d is smaller than a critical width d_c, the $E1$ subband energy is larger than the one of the $H1$ subband, and a semiconductor (SC) phase is obtained with a conventional alignment of the electronic states. Above d_c, the $E1$ subband drops below the $H1$ subband and the 2D TI phase is formed by this inverted band ordering [12,13]. Consequently, at the critical thickness d_c, the band gap closes, establishing a topological transition between the SC and TI phases, and the QW hosts single-valley 2D massless DFs [9].

In addition to the QW thickness, hydrostatic pressure [14] and temperature [15] should also induce the transition from the SC to TI phases across the gapless state. By using temperature or pressure as a fine-tuning external parameter, one may therefore precisely adjust the QW band gap to zero and observe single-valley massless DFs in HgTe QWs. Recently, the fingerprints of a temperature-induced transition from the TI at 4.2 K to the SC phase at 300 K, measured by magnetotransport up to 30 T [16], have been shown. However, the critical temperature at which the phase transition occurs and the massless DFs are formed could not be determined by this experimental technique at high temperatures. The latter is caused by a significant deterioration of resolution between the Landau levels (LLs) observed in magnetotransport in 2D systems with increasing temperature.

One of the specific properties of massless fermions is their behavior in a perpendicular magnetic field, which transforms a zero-field continuum of electronic states into a set of nonequidistantly spaced LLs with a square-root dependence of their energy on the magnetic field [2–8]. Recently, the ability to probe temperature-induced 3D massless fermions in HgCdTe crystals by far-infrared (FIR) magnetoabsorption spectroscopy was reported, enabling direct and accurate measurements of the Fermi velocity [7].

In this paper, we report on an observation of 2D massless DFs induced by temperature in HgTe QWs by FIR magnetospectroscopy. Previous magnetospectroscopy studies of DFs in HgTe QWs have either been performed at low temperatures [17–21] or only probed the temperature evolution of LL transitions with monochromatic terahertz (THz) light sources [22]. Here, by probing the inter- and intraband LL transitions, we explore the continuous evolution of the band structure with temperature and define a critical temperature T_c, corresponding to the emergence of 2D massless DFs and to the topological phase transition in HgTe QWs.

The two QW samples studied in this work were grown by molecular beam epitaxy on a [013]-oriented semi-insulating GaAs substrate with a relaxed CdTe buffer [23], with nominal

*frederic.teppe@umontpellier.fr

well widths d of 6 nm (sample A) and 8 nm (sample B). The HgTe QW is embedded in $Cd_xHg_{1-x}Te$ barriers with a nominal thickness of about 40 nm, $x = 0.62$ for sample A and 0.80 for sample B. A CdTe cap layer was deposited on top of the structures. The QW in sample B is remotely doped on each side by a 15-nm-thick In-doped region with a doping concentration of 6.5×10^{16} cm^{-3}, resulting in an electron concentration in the well of 3×10^{11} cm^{-2} at 2 K. Sample A is nominally undoped with a concentration of 2D holes of 3×10^{10} cm^{-2} at a low temperature.

According to the temperature-dependent band-structure calculations on the basis of the eight-band Kane Hamiltonian [14], sample A is expected to be almost gapless but with direct band ordering at 2 K, and its gap increases with temperature. It is clearly seen in Fig. 1 that the band ordering in sample B changes with temperature. The critical temperature T_c, corresponding to the phase transition, is estimated to be 90 K.

The origin of temperature-driven band ordering in HgTe/CdTe QWs is caused by a strong temperature dependence of the energy gap at the Γ point between the Γ_6 and Γ_8 bands in HgCdTe crystals [7]. Since the band gap in HgTe/CdTe QW depends on quantum confinement and, consequently, on the energy gap difference of the well and barrier materials, the variation of both temperature and QW width influences the band ordering in the QW. We note that for a quantitative description of the temperature effect on the band ordering, additionally to the gap, one should also take into account the temperature dependence of the valence band offset, the lattice constants, and the elastic constants in the bulk materials [14].

Figure 1 shows that, at 2 K, sample B is a TI with an indirect gap of about 10 meV, appearing due to the presence of four side maxima in the valence band. At the transition point, the linear band dispersion in the vicinity of the Γ point of the Brillouin zone clearly features the presence of massless DFs. At $T > T_c$, sample B is a normal direct-gap semiconductor. The bottom panels in Fig. 1 present a LL fan chart at 2, 90, and 120 K. To calculate LLs, we imply the axial approximation [14] by keeping the in-plane rotation symmetry and omitting the warping terms and also the terms resulting from bulk inversion asymmetry (BIA) of the unit cell in bulk zinc-blende crystals. In this case the electron wave function for a given LL index $n > 0$ generally has eight components, describing the contribution of the Γ_6, Γ_7, and Γ_8 bands into the LL. We note that a specific LL with $n = -2$ contains only a contribution of the heavy-hole band with a momentum projection $-\frac{3}{2}$ [17,18,24]. Details of the LL notation can be found in Ref. [14].

The inherent property of each phase is characterized by the behavior of a particular pair of LLs, so-called zero-mode LLs, under an applied magnetic field B [9,12,13]. The origin of this peculiar pair of LLs becomes apparent when using a modified 4×4 Dirac-type Hamiltonian [12] for the approximate description of electronic states at small values of quasimomentum $\mathbf{k}$. For the inverted band structure, below a critical field value B_c, the lowest zero-mode LL has an electronlike character and arises from the valence band, while the highest zero-mode LL has a heavy-hole-like character and splits from the conduction band. With increasing magnetic field, the zero-mode LLs cross each other at $B = B_c$. For direct band ordering, the zero-mode LLs are not crossed as the electron- and heavy-hole-like level arises at $B = 0$ in the conduction and valence band, respectively. Such a particular pair of zero-mode LLs is defined by the LLs with $n = -2$ and $n = 0$ and can be easily recognized in Fig. 1. In contrast, sample A remains in the SC phase with increasing temperature, and therefore their zero-mode LLs do not cross with the magnetic field [see Fig. 2(a)].

To probe the temperature evolution of the zero-mode LLs, we have performed FIR magnetotransmission measurements in the Faraday configuration by using a Fourier transform spectrometer coupled to a 16 T superconducting coil. The specific design of the experimental setup [7] allows for the continuous tuning of temperature in the range from 2 up to 150 K. The magnetoabsorption spectra were measured with a spectral resolution of 0.75 meV. All spectra were normalized by the sample transmission at zero magnetic field.

The magnetotransmission spectra of sample A at 2 and 70 K are presented in Figs. 2(b) and 2(c). The spectra for other temperatures are given in Ref. [25]. Samples are completely opaque in the range of the $Cd_xHg_{1-x}Te$ and the GaAs reststrahlen bands, indicated by shaded areas. In the Faraday configuration, optically active inter-LLs transitions follow the conventional selection rules $\Delta n = \pm 1$ (for unpolarized radiation) imposed by the electric dipole approximation. Due to the small hole concentration in sample A, only a few LLs in the valence band are occupied. For instance, $B \simeq 1.2$ T corresponds to a LL filling factor $\nu = 1$ for the concentration at 2 K. Therefore, three high-intensity lines in the spectra for all temperatures can be identified as inter-band LL transitions, involving the zero-mode LLs. Those transitions are marked in Fig. 2(a) with lowercase greek letters, in accordance with previously used notations [17–20].

A comparison of the experimental and theoretical values of the transition energies is presented in Fig. 2(d). We note that extrapolation of the energy behavior in magnetic field of the inter-band LL transitions into $B = 0$ allows for the evaluation of the band gap at zero quasimomentum. A very good agreement of the experimental data with theoretical calculations clearly demonstrates the band-gap opening in sample A, induced by temperature. The latter is indicated in Fig. 2(d) by blue arrows.

Figure 3 presents the magnetotransmission spectra of sample B at 2, 90, and 130 K (the top panels). The spectra for other temperatures are given in Ref. [25]. The three most intense lines observed at all temperatures are identified as the LL transitions from the zero-mode LLs (α and β transitions) and cyclotron resonance (CR) absorption due to 2D electrons (γ and δ transitions). By using the electron concentration at 2 K, one concludes that CR in the fields below 3.4 T, corresponding to $\nu \approx 3$, can be related to both γ and δ transitions, while above this field only a γ transition is possible. It is seen that the γ line disappears from the spectrum at $B \approx 12$ T. Assuming that $B = 12$ T corresponds to $\nu = 1$, we find an excellent agreement upon the electron concentration, previously derived from magnetotransport measurements.

At 2 K, an additional α' transition, shown in Fig. 1, appears in the spectra in a relatively narrow range of magnetic fields $B = 5$–7.5 T, in which the zero-mode LLs are crossed. Such a transition does not satisfy the selection rules $\Delta n = \pm 1$ and is

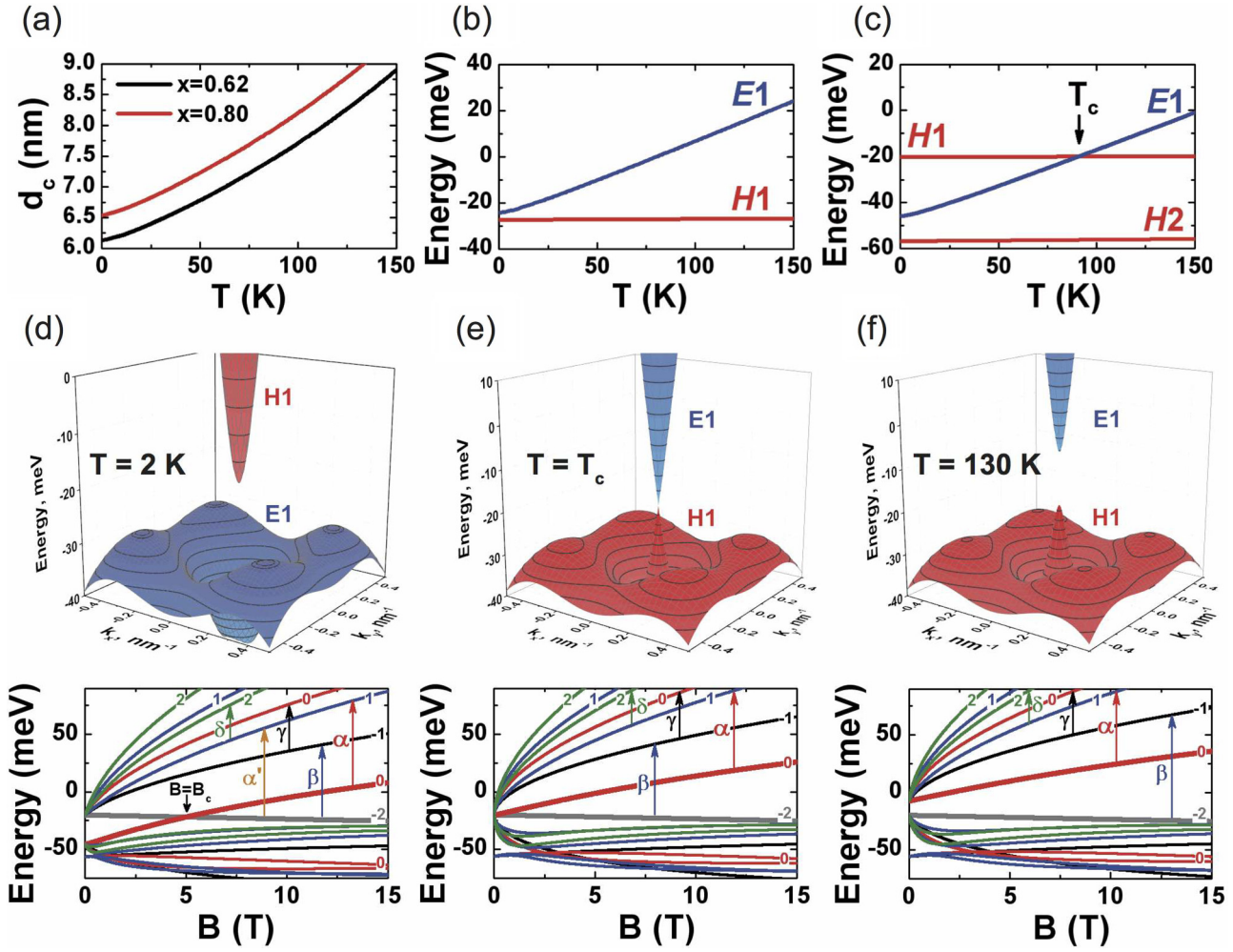

FIG. 1. (a) Critical QW width d_c, corresponding to the phase transition and emergence of massless Dirac fermions, as a function of temperature in (013) HgTe/Cd$_x$Hg$_{1-x}$Te QWs for $x = 0.62$ and 0.80. (b), (c) Temperature dependence of the electronlike $E1$ and the heavy-hole-like $H1, H2$ subbands as a function of temperature at zero quasimomentum (b) for sample A and (c) sample B. (d)–(f) Band structure (top panels) and Landau levels (bottom panels) in sample B at different temperatures: (d) $T = 2$ K, (e) $T = T_c$, and (f) $T = 130$ K. The $E1$ subband in the top panels is shown in blue, and the red surface corresponds to the $H1$ subband. The x and y axes are oriented along the (100) and (03$\bar{1}$) crystallographic directions, respectively. The numbers over the curves in the bottom panels correspond to the LL indices. A pair of zero-mode LLs with indices -2 and 0 is shown by bold curves. The arrows and greek letters denote LL transitions, observed in the magnetoabsorption spectra of sample B.

forbidden in the electric dipole approximation. The emergence of this transition, also previously reported in Refs. [17–19], is related to the coupling between the $n = 0$ and $n = -2$ LLs, resulting from BIA, initially neglected in our calculations. Taking into account BIA leads to anticrossing in the vicinity of $B = B_c$ and to the mixing of the states at the zero-mode LLs. The latter makes the α' transition become active in the electric dipole approximation. The observation of the α' line, which is followed up to 30 K in our data, is direct evidence of the inverted band structure of sample B at low temperatures.

As it has been mentioned above, a distinctive characteristic of massless particles is the square-root dependence of the energies of LL transitions on the magnetic field [2–8]. However, linear subband dispersion in HgTe QWs exists only in the vicinity of the Γ point. At large values of quasimomentum k, the terms, proportional to k^2, in the Hamiltonian become relevant [12,13]. The latter give rise to the square-root behavior in weak magnetic fields only, while at high magnetic fields, the linear dependence should be seen. This can be shown by straightforward calculations on the basis of the eight-band Kane Hamiltonian [25].

A more representative characteristic of the gapless state in HgTe QWs is the behavior of the transitions from the zero-mode LLs. If the band structure is inverted, the energy of the α transition leans towards the gap energy at $k = 0$ when B tends to zero, while the energy of the β transition vanishes. For direct band ordering, the transition behavior in weak magnetic fields is reversed: The gap at $k = 0$ corresponds to the cutoff energy for the β transition, however, the energy of the α transition tends to zero. In the gapless state with 2D massless DFs, the energy of both transitions should have the same dependence on B in weak magnetic fields, and the corresponding absorption lines merge if the magnetic field goes to zero. The latter is seen in the transmission spectra at 90 K, which indicates a vanishing of the gap at $k = 0$ and hence the emergence of 2D massless DFs.

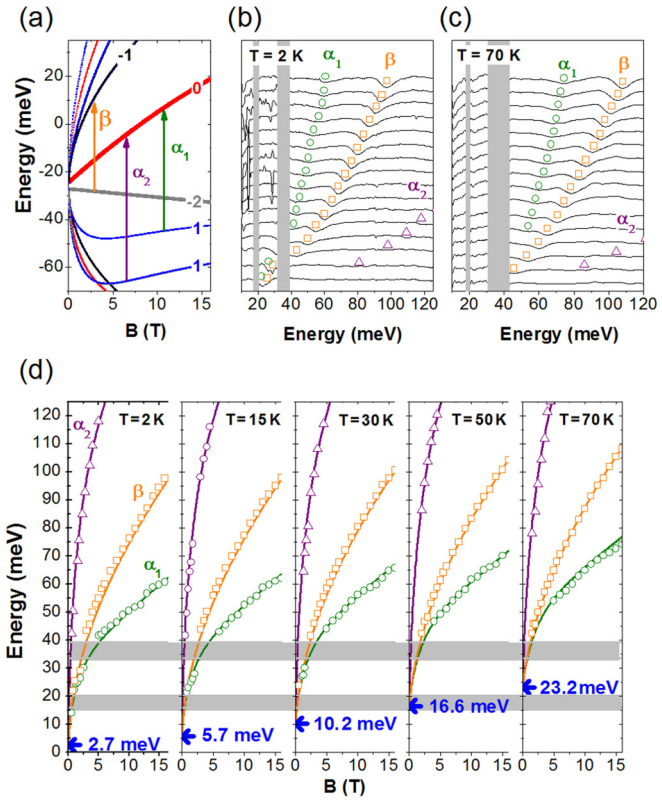

FIG. 2. (a) LLs as a function of magnetic field in sample A at 2 K. The numbers conform to the LL indices. The zero-mode LLs are shown by bold curves. The arrows and greek letters denote LL transitions, observed in the magnetoabsorption spectra. (b), (c) Transmission spectra of sample A at 2 and 70 K from 1 T (the first plot at the bottom) to 16 T (the last plot on the top) with a step for the magnetic field of 1.0 T. (d) Energy of α_1 (green curve), α_2 (purple curve), and β (orange curve) transitions as a function of magnetic field. The experimental data are represented by symbols: circles, triangles, and squares for the α_1, α_2, and β transitions, respectively. The value of the band gap is shown by blue arrows. Shaded areas indicate the reststrahlen bands, although in order to simplify the figure, their evolution with temperature has not been represented here. For simplicity, the evolution of the reststrahlen bands with temperature is not shown in the panel.

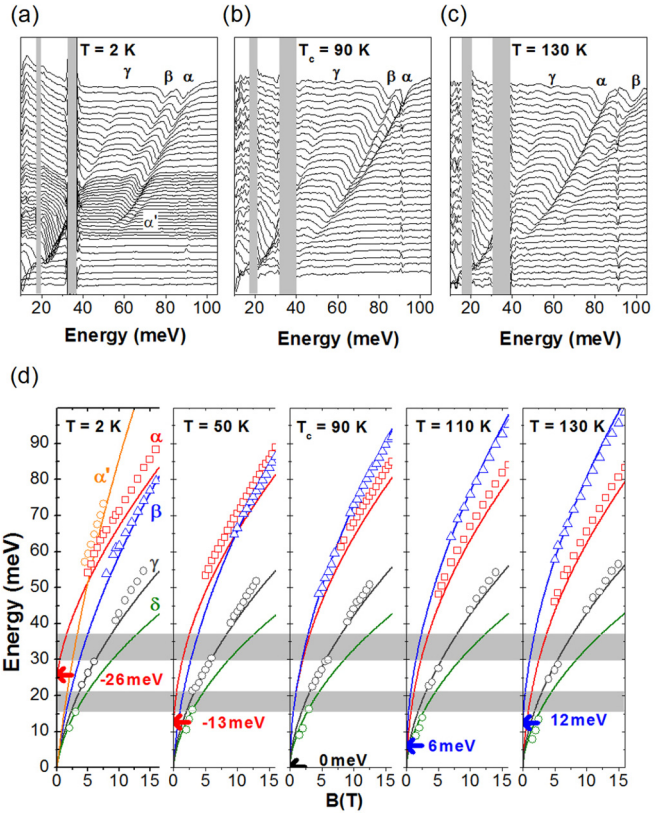

FIG. 3. (a)–(c) Transmission spectra of sample B at 2, 90, and 130 K from 0.5 T (the first plot at the bottom) to 16 T (the last plot on the top). The step for the magnetic field is 0.5 T, except for the 2 K panel, in which a 0.25 T step was used between 4 and 9 T, allowing one to accurately follow the evolution of the α' transition. The greek letters denote LL transitions, shown in Fig. 1. (d) Fan chart of inter-LL transitions in sample B. The α', α, β, γ, and δ calculated transitions are shown in solid lines in orange, red, dark gray, and green, respectively. Experimental data are represented by symbols in the same colors as the theoretical curves. The gap at $k = 0$ is shown by blue and red arrows, respectively, for negative and positive values, and black for the gapless state. Shaded areas indicate the reststrahlen bands, although in order to simplify the figure, their evolution with temperature has not been represented here. For simplicity, the evolution of the reststrahlen bands with temperature is not shown.

We note that the merging of α and β lines with decreasing magnetic field in the gapless state can also be derived analytically from a modified 4×4 Dirac-type 2D Hamiltonian [12], also used for the description of previous magnetotransport results on 2D massless DFs [9]. Unfortunately, the large number of variable parameters of this 2D model does not allow us to use it for efficient fitting of the experimental data. As a result, only the observation of the α and β LL transition behaviors in the transmission spectra makes it possible to demonstrate the band-gap vanishing and to determine the critical temperature T_c, while the band velocity v_F of massless DFs cannot be directly extracted from the data. However, a good agreement between theoretical calculations and experimental data for sample B evidences that the actual band velocity of massless DFs at 90 K should be very close to the theoretical value $v_F = 5.6 \times 10^5$ m s^{-1} [25].

In conclusion, we have demonstrated the ability to observe a change in the band gap in HgTe QWs by temperature-dependent FIR magnetotransmission spectroscopy. In the case of an inverted band structure, we have determined a critical temperature $T_c = 90$ K, corresponding to the band-gap vanishing and hence the emergence of single-valley 2D massless DFs. A good agreement between experimental results and theoretical calculations on the basis of the eight-band Kane Hamiltonian with temperature-dependent parameters allows us to evaluate the band velocity of 2D massless DFs.

This work was supported by the Languedoc-Roussillon region via the "Gepeto Terahertz platform" and the ARPE project "Terasens", by the CNRS through the Emergence project 2016, and through the LIA "TeraMIR" project, by MIPS department of Montpellier University through the "Occitanie Terahertz Platform", by the Foundation for Polish Science through the grant TEAM, by the Eranet-Rus-Plus European program "Terasens", by the Russian Academy of Sciences, by

the Russian Foundation for Basic Research (Grants No. 15-52-16017 and No. 16-02-00672), and by the Russian Ministry of Education and Science (MK-1136.2017.2). Theoretical calculations and characterization of the samples were performed in the framework of Project No. 16-12-10317 provided by the Russian Science Foundation.

[1] T. O. Wehling, A. M. Black-Schaffer, and A. V. Balatsky, Adv. Phys. **63**, 1 (2014).
[2] K. S. Novoselov, A. K. Geim, S. V. Morozov, D. Jiang, M. I. Katsnelson, I. V. Grigorieva, S. V. Dubonos, and A. A. Firsov, Nature (London) **438**, 197 (2005).
[3] Y. Zhang, Y.-W. Tan, H. L. Stormer, and P. Kim, Nature (London) **438**, 201 (2005).
[4] M. Z. Hasan and C. L. Kane, Rev. Mod. Phys. **82**, 3045 (2010).
[5] Z. K. Liu, J. Jiang, B. Zhou, Z. J. Wang, Y. Zhang, H. M. Weng, D. Prabhakaran, S.-K. Mo, H. Peng, P. Dudin, T. Kim, M. Hoesch, Z. Fang, X. Dai, Z. X. Shen, D. L. Feng, Z. Hussain, and Y. L. Chen, Nat. Mater. **13**, 677 (2014).
[6] M. Orlita, D. M. Basko, M. S. Zholudev, F. Teppe, W. Knap, V. I. Gavrilenko, N. N. Mikhailov, S. A. Dvoretskii, P. Neugebauer, C. Faugeras, A.-L. Barra, G. Martinez, and M. Potemski, Nat. Phys. **10**, 233 (2014).
[7] F. Teppe, M. Marcinkiewicz, S. S. Krishtopenko, S. Ruffenach, C. Consejo, A. M. Kadykov, W. Desrat, D. But, W. Knap, J. Ludwig, S. Moon, D. Smirnov, M. Orlita, Z. Jiang, S. V. Morozov, V. Gavrilenko, N. N. Mikhailov, and S. A. Dvoretskii, Nat. Commun. **7**, 12576 (2016).
[8] S.-Y. Xu, I. Belopolski, N. Alidoust, M. Neupane, G. Bian, C. Zhang, R. Sankar, G. Chang, Z. Yuan, C.-C. Lee, S.-M. Huang, H. Zheng, J. Ma, D. S. Sanchez, B. Wang, A. Bansil, F. Chou, P. P. Shibayev, H. Lin, S. Jia, and M. Z. Hasan, Science **349**, 613 (2015).
[9] B. Büttner, C. Liu, G. Tkachov, E. Novik, C. Brüne, H. Buhmann, E. Hankiewicz, P. Recher, B. Trauzettel, S. Zhang, and L. Molenkamp, Nat. Phys. **7**, 418 (2011).
[10] Y. R. Lin-Liu and L. J. Sham, Phys. Rev. B **32**, 5561 (1985).
[11] L. G. Gerchikov and A. V. Subashiev, Phys. Status Solidi B **160**, 443 (1990).
[12] B. A. Bernevig, T. L. Hughes, and S.-C. Zhang, Science **314**, 1757 (2006).
[13] M. König, S. Wiedmann, C. Brüne, A. Roth, H. Buhmann, L. W. Molenkamp, X.-L. Qi, and S.-C. Zhang, Science **318**, 766 (2007).
[14] S. S. Krishtopenko, I. Yahniuk, D. B. But, V. I. Gavrilenko, W. Knap, and F. Teppe, Phys. Rev. B **94**, 245402 (2016).
[15] P. Sengupta, T. Kubis, Y. Tan, M. Povolotskyi, and G. Klimeck, J. Appl. Phys. **114**, 043702 (2013).
[16] S. Wiedmann, A. Jost, C. Thienel, C. Brüne, P. Leubner, H. Buhmann, L. W. Molenkamp, J. C. Maan, and U. Zeitler, Phys. Rev. B **91**, 205311 (2015).
[17] M. Orlita, K. Masztalerz, C. Faugeras, M. Potemski, E. G. Novik, C. Brüne, H. Buhmann, and L. W. Molenkamp, Phys. Rev. B **83**, 115307 (2011).
[18] M. Zholudev, F. Teppe, M. Orlita, C. Consejo, J. Torres, N. Dyakonova, M. Czapkiewicz, J. Wróbel, G. Grabecki, N. Mikhailov, S. Dvoretskii, A. Ikonnikov, K. Spirin, V. Aleshkin, V. Gavrilenko, and W. Knap, Phys. Rev. B **86**, 205420 (2012).
[19] J. Ludwig, Y. B. Vasilyev, N. N. Mikhailov, J. M. Poumirol, Z. Jiang, O. Vafek, and D. Smirnov, Phys. Rev. B **89**, 241406 (2014).
[20] M. S. Zholudev, F. Teppe, S. V. Morozov, M. Orlita, C. Consejo, S. Ruffenach, W. Knap, V. I. Gavrilenko, S. A. Dvoretskii, and N. N. Mikhailov, JETP Lett. **100**, 790 (2015).
[21] A. M. Kadykov, J. Torres, S. S. Krishtopenko, C. Consejo, S. Ruffenach, M. Marcinkiewicz, D. But, W. Knap, S. V. Morozov, V. I. Gavrilenko, N. N. Mikhailov, S. A. Dvoretsky, and F. Teppe, Appl. Phys. Lett. **108**, 262102 (2016).
[22] A. V. Ikonnikov, S. S. Krishtopenko, O. Drachenko, M. Goiran, M. S. Zholudev, V. V. Platonov, Y. B. Kudasov, A. S. Korshunov, D. A. Maslov, I. V. Makarov, O. M. Surdin, A. V. Philippov, M. Marcinkiewicz, S. Ruffenach, F. Teppe, W. Knap, N. N. Mikhailov, S. A. Dvoretsky, and V. I. Gavrilenko, Phys. Rev. B **94**, 155421 (2016).
[23] S. Dvoretsky, N. Mikhailov, Y. Sidorov, V. Shvets, S. Danilov, B. Wittman, and S. Ganichev, J. Electron. Mater. **39**, 918 (2010).
[24] S. S. Krishtopenko, W. Knap, and F. Teppe, Sci. Rep. **6**, 30755 (2016).
[25] See Supplemental Material at http://link.aps.org/supplemental/10.1103/PhysRevB.96.035405 for additional magnetotransmission spectra and a brief discussion of the Dirac-type 2D Hamiltonian, which includes Refs. [26,27].
[26] S. A. Tarasenko, M. V. Durnev, M. O. Nestoklon, E. L. Ivchenko, J.-W. Luo, and A. Zunger, Phys. Rev. B **91**, 081302 (2015).
[27] M. König, H. Buhmann, L. W. Molenkamp, T. Hughes, C.-X. Liu, X.-L. Qi, and S.-C. Zhang, J. Phys. Soc. Jpn. **77**, 031007 (2008).